THREE-DIMENSIONAL ANALYSIS OF ELASTIC BEHAVIOR OF WOOD FIBER[1]

R. C. Tang

Department of Forestry, University of Kentucky, Lexington, Kentucky 40506

(Received 28 January 1971)

ABSTRACT

An exact solution of stress for each layer of cell wall under tension has been obtained by considering wood fiber as a hollow composite anisotropic circular cylinder. Numerical results of stresses and the relative angle of twist of a single fiber, as well as the values of each layer of the cell wall, are given for six hypothetical wood fibers.

Notation

$\sigma_k^{(j)}$	Normal stress in jth layer
$\sigma_{kl}^{(j)}$	Shear stress in jth layer
P	Tensile force at ends
a_j	Radius of fiber at the outer edge of jth layer
$A,B,C,D,$ E,F	Unknown constants
$a_{mn}^{(j)}$	Compliances of jth layer
$\beta_{mn}^{(j)}$	Coefficients of deformation of jth layer
$u_k^{(j)}$	Displacement in jth layer
E_i	Young's moduli
G_{ij}	Moduli of rigidity
μ_{ij}	Directional Poisson's ratios
T	Torsional rigidity of a single fiber
$T^{(j)}$	Torsional rigidity of jth layer
D_{total}	Total relative angle of twist of a single fiber
Φ,Ψ	Stress functions

INTRODUCTION

In recent years, considerable effort has been expended in the development of fiber mechanics, and as a consequence, the mechanical behavior of the cell wall has become very important. The problems in general may be classified as follows: (1) determination of the elastic constants of crystalline cellulose on the microscopic level; (2) determination of the elastic constants of the cell wall on the microscopic level; and (3) stress distribution on each layer of the cell wall when the fiber is deformed.

The first problem has been extensively studied by many authors (Gillis 1969; Gillis, Mark, and Tang 1969; Jaswon, Gillis, and Mark 1968; Lyons 1959; Mark et al. 1969; Meredith 1946; Sakusada, Nukushina, and Ito 1962; Treloar 1960). In dealing with the second problem, several authors have used the concept of layered system (Cave 1968; 1969; Gillis 1970; Mark 1967; Mark and Gillis 1970; Schniewind 1969; Schniewind and Barrett 1969). Literature in the third category, however, is limited. As is known, the theoretical study of stress in each layer of the cell wall is restricted in two-dimensional analysis by cutting an element from the wall of tubular wood fiber (Mark 1967; Mark and Gillis 1970; Schniewind 1969; Schniewind and Barrett 1969). It is quite obvious that a significant change of stress in each layer of the wall will arise when considered as a three-dimensional system. This has been demonstrated by the experimental testing of a helically reinforced plastics pipe (Mark 1967). The rotation test of a simple fiber (pine) under tension has been reported by Mark and Gillis (1970). No literature on the theoretical analysis of twisting of a single fiber has been found by the author.

In this paper, the stresses and the relative angle of twist on each layer of cell wall are

[1] The investigation reported in this paper (No. 71-8-13) is in connection with a project of the Kentucky Agricultural Experiment Station and is published with the approval of the Director. Funds for this research were made available under the provision of the McIntire-Stennis Cooperative Forestry Research Program of the U. S. Department of Agriculture. The author is indebted to this agency and to the Kentucky Agricultural Experiment Station for their support on this project. The numerical analysis was completed on the facilities at the University of Kentucky computing center.

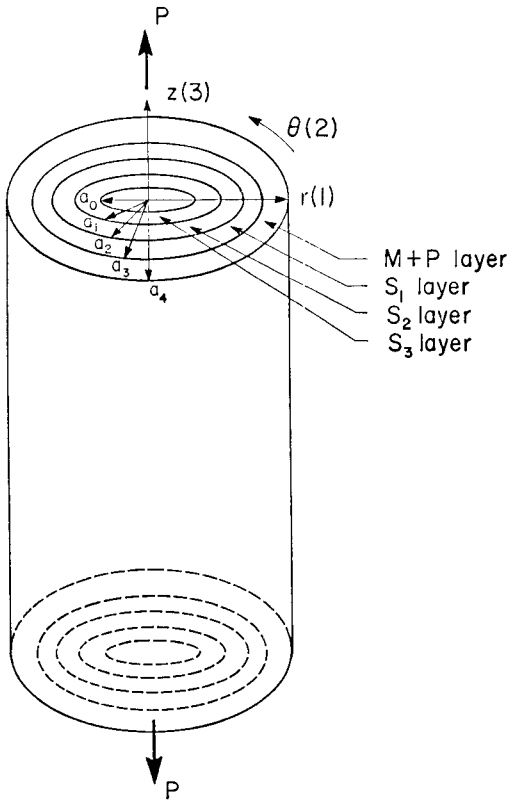

FIG. 1. Schematic diagram of the problem.

calculated by considering the wood fiber as a hollow composite anisotropic circular cylinder subjected to tension. It is desirable to model the fiber as a cylinder of rectangular or a square cross section, possessing two different sets of elastic constants for the tangential and radial walls. To obtain more precise results, it would be desirable to round corners in a manner to simulate the geometry of a fiber. The analysis of such a cylinder is very complex, however. Consequently, in this work the fiber was assumed to be of circular cross section. Such an approach will yield results more nearly consistent with the actual behavior of the fiber than the two-dimensional analysis reported to date.

THE BASIC EQUATIONS AND SOLUTION

Let us consider wood fiber as a composite anisotropic cylinder of finite length, made from a material with cylindrical anisotropy, and subjected to a tensile force P at the ends (Fig. 1). We assume that: (1) the axis of anisotropy coincides with the geometric axis of the cylinder, and (2) the stresses that act on the end surfaces reduce to forces and to twisting moments directed along the axis.

According to Lekhnitskii (1963), the governing partial differential equations of a hollow cylinder with body forces absent take the forms:

$$L'_4\Phi + L'_3\Psi = 0,$$
$$L''_3\Phi + L'_2\Psi = \frac{Fa_{34}}{r} - 2D \qquad (1)$$

Here F is an arbitrary constant, a_{34} is an elastic constant, D is the relative angle of twist, and L'_2, L'_3, L''_3, L'_4 are differential operators defined as follows:

$$L'_2 = \beta_{44}\frac{\partial^2}{\partial r^2} + \beta_{55}\frac{1}{r^2}\frac{\partial^2}{\partial\theta^2} + \beta_{44}\frac{1}{r}\frac{\partial}{\partial r},$$

$$L'_3 = -\beta_{24}\frac{\partial^3}{\partial r^3} - \beta_{14}\frac{1}{r^2}\frac{\partial^3}{\partial r\partial\theta^2} + \left(\beta_{14}-2\beta_{24}\right)\frac{1}{r}\frac{\partial^2}{\partial r^2},$$

$$L''_3 = -\beta_{24}\frac{\partial^3}{\partial r^3} - \beta_{14}\frac{1}{r^2}\frac{\partial^3}{\partial r\partial\theta^2} - \left(\beta_{14}+\beta_{24}\right)\frac{1}{r}\frac{\partial^2}{\partial r^2} + \beta_{14}\frac{1}{r^3}\frac{\partial^2}{\partial\theta^2},$$

$$L'_4 = \beta_{22}\frac{\partial^4}{\partial r^4} + \left(2\beta_{12}+\beta_{66}\right)\frac{1}{r^2}\frac{\partial^4}{\partial r^2\partial\theta^2} + \beta_{11}\frac{1}{r^4}\frac{\partial^4}{\partial\theta^4} + 2\beta_{22}\frac{1}{r}\frac{\partial^3}{\partial r^3} - \left(2\beta_{12}+\beta_{66}\right)\frac{1}{r^3}\frac{\partial^3}{\partial r\partial\theta^2} - \beta_{11}\frac{1}{r^2}\frac{\partial^2}{\partial r^2} + \left(2\beta_{11}+2\beta_{12}+\beta_{66}\right)\frac{1}{r^4}\frac{\partial^2}{\partial\theta^2} + \beta_{11}\frac{1}{r^3}\frac{\partial}{\partial r} \qquad (2)$$

where β_{mn}'s are the elastic coefficients of deformations.

Because the stress distribution in a hollow cylinder is symmetrical about the center axis, the stress functions Φ and Ψ will depend only on the radius r (Tang and Adams 1970). Assuming plane deformation of a composite cylinder (Fig. 1), then equations (1) are satisfied if we take the stress components of the jth layer in the following form:

$$\sigma_r^{(j)} = \frac{\Phi'(r)^{(j)}}{r} = E^{(j)}\frac{\beta_{14}^{(j)}}{\beta_{44}^{(j)}} r^{-1} + A^{(j)} + B^{(j)} r^{k_j - 1} + C^{(j)} r^{-k_j - 1} + D^{(j)} G^{(j)} r , \quad (3)$$

$$\sigma_\theta^{(j)} = \Phi''(r)^{(j)} = A^{(j)} + B^{(j)} K_j r^{k_j - 1} - C^{(j)} k_j r^{-k_j - 1} + 2D^{(j)} G^{(j)} r , \quad (4)$$

$$\sigma_{\theta z}^{(j)} = \Psi'(r)^{(j)} = -E^{(j)} - F^{(j)}\frac{a_{34}^{(j)}}{\beta_{44}^{(j)}} - A^{(j)} g_1^{(j)} - B^{(j)} g_k^{(j)} r^{k_j - 1} - C^{(j)} g_{-k}^{(j)} r^{-k_j - 1} + D^{(j)} H^{(j)} r , \quad (5)$$

$$\sigma_z^{(j)} = F^{(j)} - \frac{1}{a_{33}^{(j)}}\left(a_{13}^{(j)}\sigma_r^{(j)} + a_{23}^{(j)}\sigma_\theta^{(j)} + a_{34}^{(j)}\sigma_{\theta z}^{(j)} \right) \quad (6)$$

$$\sigma_{r\theta}^{(j)} = \sigma_{rz}^{(j)} = 0 \quad (7)$$

Here all the superscripts (j) or the subscripts (j) indicate particular layers. $A^{(j)}$ $B^{(j)}$, $C^{(j)}$, $D^{(j)}$, $E^{(j)}$, $F^{(j)}$ are the arbitrary constants to be determined from boundary conditions, and $D^{(j)}$ is the constant equal to the relative angle of twist. The constants a_{mn} are the elastic coefficients of the material. Other constants are as follows:

$$\beta_{mn}^{(j)} = \left[a_{mn} - \frac{a_{m3}a_{n3}}{a_{33}} \right]_j \quad (m,n = 1,2,4,5,6); \quad (a)$$

$$k_j = \left[\frac{\beta_{11}\beta_{44} - \beta_{14}^2}{\beta_{22}\beta_{44} - \beta_{24}^2} \right]_j^{1/2}; \quad (b)$$

$$g_{\pm k}^{(j)} = \left[\frac{\beta_{14} \pm k\beta_{24}}{\beta_{44}} \right]_j , \quad (\text{in particular } g^{(j)} = \left[\frac{\beta_{14} + \beta_{24}}{\beta_{44}}\right]_j); \quad (c)$$

$$G^{(j)} = \left[\frac{\beta_{14} - 2\beta_{24}}{4(\beta_{22}\beta_{44} - \beta_{24}^2) - (\beta_{11}\beta_{44} - \beta_{14}^2)} \right]_j ; \quad (d)$$

$$H^{(j)} = -\left[\frac{\beta_{11} - 4\beta_{22}}{4(\beta_{22}\beta_{44} - \beta_{24}^2) - (\beta_{11}\beta_{44} - \beta_{14}^2)} \right]_j . \quad (e)(8)$$

It follows from equations (3–7) that the displacements in jth layer can be expressed as

$$u_r^{(j)} = \int (a_{11}^{(j)}\sigma_r^{(j)} + a_{12}^{(j)}\sigma_\theta^{(j)} + a_{13}^{(j)}\sigma_z^{(j)} + a_{14}^{(j)}\sigma_{\theta z}^{(j)}) \, dr ,$$

$$u_\theta^{(j)} = \int (a_{14}^{(j)}\sigma_r^{(j)} + a_{24}^{(j)}\sigma_\theta^{(j)} + a_{34}^{(j)}\sigma_z^{(j)} + a_{44}^{(j)}\sigma_{\theta z}^{(j)}) \, dz . \quad (9)$$

The boundary conditions on the cylindrical surfaces are as follows:

$$\sigma_r^{(1)} = 0 \quad \text{at} \quad r = a_0$$
$$\text{and} \quad \sigma_r^{(4)} = 0 \quad \text{at} \quad r = a_4 \quad (10)$$

At the contact surfaces of adjacent layers, the following stress and displacement relations must hold:

$$\sigma_r^{(j)} = \sigma_r^{(j+1)} ;$$
$$u_r^{(j)} = u_r^{(j+1)} ;$$
$$\sigma_{\theta z}^{(j)} = \sigma_{\theta z}^{(j+1)} . \quad (11)$$

The boundary conditions for $r = a_j$ ($j = 1, 2, 3$) at the ends are

$$\sum_{j=1}^{4} \int_{a_{j-1}}^{a_j} \sigma_z^{(j)} r \, dr = \frac{p}{2\pi} , \quad \text{and}$$
$$\sum_{j=1}^{4} \int_{a_{j-1}}^{a_j} \sigma_{\theta z}^{(j)} r^2 dr = 0 . \quad (12)$$

In determining displacements and requiring that they be a single-valued function of the coordinates, it is necessary that:

$$E^{(j)} = 0$$

$$\text{and} \quad A^{(j)} = F^{(j)}h^{(j)} \tag{13}$$

$$\text{where} \quad h^{(j)} = \left[\frac{(a_{13}-a_{23})\beta_{44} - a_{34}(\beta_{14}-\beta_{24})}{\beta_{22}\beta_{44}-\beta_{24}^2-(\beta_{11}\beta_{44}-\beta_{14}^2)}\right]_j.$$

It should be noted also that:

$$F^{(j)} = F^{(j+1)} = F.$$

For the generalized plane deformation problems, the axial strain is constant.

$$\frac{\partial \omega}{\partial z} = \text{constant}.$$

Consequently, when a composite cylinder is subjected to a tensile force P at the ends, the axial strain of all layers must be identical; hence:

$$\frac{\partial \omega^{(j)}}{\partial z} = \frac{\partial \omega^{(j+1)}}{\partial z} = F.$$

Using the boundary conditions given in (10), we obtain:

$$Fh^{(1)} + B^{(1)}a_o^{k_1-1} + C^{(1)}a_o^{-k_1-1} + D^{(1)}G^{(1)}a_o = 0. \tag{14}$$

$$Fh^{(4)} + B^{(4)}a_4^{k_4-1} + C^{(4)}a_4^{-k_4-1} + D^{(4)}G^{(4)}a_4 = 0. \tag{15}$$

Furthermore, the boundary conditions of (11) give

$$F(h^{(j+1)}-h^{(j)}) + B^{(j+1)}a_j^{k_{j+1}-1} - B^{(j)}a_j^{k_j-1} + C^{(j+1)}a_j^{-k_{j+1}-1} - C^{(j)}a_j^{-k_j-1} + a_j(D^{(j+1)}G^{(j+1)} - D^{(j)}G^{(j)}) = 0, \ (j=1,2,3) \tag{16}$$

$$F(M_1^{(j+1)}-M_1^{(j)})a_j + B^{(j+1)}M_2^{(j+1)}\frac{a_j^{k_j+1}}{k_j+1} - B^{(j)}M_2^{(j)}\frac{a_j^{k_j}}{k_j} - C^{(j+1)}M_3^{(j+1)}\frac{a_j^{-k_j+1}}{k_j+1} + C^{(j)}M_3^{(j)}\frac{a_j^{-k_j}}{k_j} + (D^{(j+1)}M_4^{(j+1)} - D^{(j)}M_4^{(j)})\frac{a_j^2}{2} = 0, \ (j=1,2,3) \tag{17}$$

where $M_1 = (\beta_{11}+\beta_{12}-\beta_{14}g_1)h + (a_{13}-\beta_{14}\frac{a_{34}}{\beta_{44}})$,

$$M_2 = \beta_{11} + \beta_{12}k - \beta_{14}g_k,$$

$$M_3 = \beta_{11} - \beta_{12}k - \beta_{14}g_{-k},$$

$$M_4 = (\beta_{11}+2\beta_{12})G + \beta_{14}H,$$

and

$$F\left(\frac{a_{34}^{(j+1)}}{\beta_{44}^{(j+1)}} - \frac{a_{34}^{(j)}}{\beta_{44}^{(j)}} + h^{(j+1)}g_1^{(j+1)} - h^{(j)}g_1^{(j)}\right) + B^{(j+1)}g_k^{(j+1)}a_j^{k_{j+1}-1} - B^{(j)}g_k^{(j)}a_j^{k_j-1} + C^{(j+1)}g_{-k}^{(j+1)}a_j^{-k_{j+1}-1} - C^{(j)}g_{-k}^{(j)}a_j^{-k_j-1} - (D^{(j+1)}H^{(j+1)} - D^{(j)}H^{(j)})a_j = 0, \ (j=1,2,3) \tag{18}$$

From the boundary conditions given in (12), we have:

$$\sum_{j=1}^{4}\left\{\frac{F}{3}\left(\frac{a_{34}^{(j)}}{\beta_{44}^{(j)}} + h^{(j)}g_1^{(j)}\right)(a_j^3 - a_{j-1}^3) + B^{(j)}g_k^{(j)}\left(\frac{a_j^{k_j+2}-a_{j-1}^{k_j+2}}{k_j+2}\right) + C^{(j)}g_{-k}^{(j)}\left(\frac{a_j^{-k_j+2}-a_{j-1}^{-k_j+2}}{2-k_j}\right) - \frac{D^{(j)}H^{(j)}}{4}(a_j^4 - a_{j-1}^4)\right\} = 0. \tag{19}$$

and

$$\sum_{j=1}^{4}\left\{\frac{F}{2}\left[1 - \frac{1}{a_{33}^{(j)}}(a_{13}^{(j)} + a_{23}^{(j)} - a_{34}^{(j)}g_1^{(j)})h^{(j)} + \frac{\left[a_{34}^{(j)}\right]^2}{a_{33}^{(j)}\beta_{44}^{(j)}}\right](a_j^2 - a_{j-1}^2) - \frac{B^{(j)}}{a_{33}^{(j)}}\left[a_{13}^{(j)} + a_{23}^{(j)}k^{(j)} - a_{34}^{(j)}g_k^{(j)}\right]\frac{a_j^{k_j+1} - a_{j-1}^{k_j+1}}{k_j+1} - \frac{C^{(j)}}{a_{33}^{(j)}}\left[a_{13}^{(j)} - a_{23}^{(j)}k^{(j)} - a_{34}^{(j)}g_{-k}^{(j)}\right]\frac{(a_j^{-k_j+1} - a_{j-1}^{-k_j+1})}{1-k_j} -$$

$$\frac{D^{(j)}}{3a_{33}^{(j)}}\left[(a_{13}^{(j)}+2a_{23}^{(j)})G^{(j)}+a_{34}^{(j)}H^{(j)}\right](a_j^3-a_{j-1}^3)\Big\} = \frac{P}{2\pi}. \quad (20)$$

These unknown constants $B^{(j)}$, $C^{(j)}$, $D^{(j)}$, ($j = 1, 2, 3, 4,$) and F can be determined from equations (14)–(20). Consequently, all the data necessary for calculation of stresses and displacements are available.

NUMERICAL EXAMPLES

It is known that the microfibrillar angles in S_2 and S_3 layers on the tangential wall of wood fiber are different from those on the radial wall except in the S_1 layer and $M + P$ layer (middle lamella and primary wall). The variation of these microfibrillar angles and the area percentage of the various cell-wall layers in the fiber are listed in Table 1 (Mark and Gillis 1970).

To simplify the numerical calculations, models were used with structure configurations as listed in Table 2. Assuming that the exterior radius of each model is a unity, then, according to Table 2, the corresponding radius of each layer is found to be:

a_0	(to the inner edge of S_3):	0.82566
a_1	(to the inner edge of S_2):	0.84700
a_2	(to the inner edge of S_1):	0.95643
a_3	(to the inner edge of $M + P$):	0.98396
a_4	(to the outer edge of $M + P$):	1.00000

The elastic constants of each layer were calculated by using an approach similar to that of Gillis (1970). Three cases are considered. The elastic constants of crystalline cellulose are listed in Table 3.

TABLE 1. *Microfibril angles and area percentages of the various cell-wall layers in the fiber*

Layer	Filament winding angles	Area % of the various cell-wall layers
Radial wall		
$M + P$	90°	7.40
S_1	± 80°	11.84
S_2	36°	45.88
S_3	64°	8.88
Tangential wall		
$M + P$	90°	2.60
S_1	± 80°	4.94
S_2	20°	16.12
S_3	30°	2.34

TABLE 2. *Data for model fibers*

Model	Layer	Filament winding angles	Area % of the various cell-wall layers
I	$M + P$	90°	10.00
	S_1	± 80°	16.78
	S_2	36°	62.00
	S_3	64°	11.22
II	$M + P$	90°	10.00
	S_1	± 80°	16.78
	S_2	20°	62.00
	S_3	30°	11.22

The values used to describe the associated matrix material and the proportions of matrix and framework in each layer are as given by Mark and Gillis (1970), viz.

$E = 0.200 \times 10^{11}$ dynes/cm^2
$G = 0.0769 \times 10^{11}$ dynes/cm^2
$\mu = 0.30$

and	Matrix (%)	Framework (%)
$M + P$	89.9	10.1
S_1, S_2 and S_3	46.9	53.1

TABLE 3. *Elastic constants of crystalline cellulose in the cell wall (E and G in units of 10^{11} dynes/cm^2)**

Case	E_1	E_2	E_3	G_{12}	G_{13}	G_{23}	μ_{12}	μ_{13}	μ_{23}	Ref
1	5.13	5.65	1.68	0.049	0.236	0.018	0.0336	–0.0016	0.041	3,6
2	2.49	31.90	3.73	0.023	0.323	0.039	0.003	–0.0002	0.041	3,5
3	2.72	13.40	2.72	0.440	0.660	0.440	0.100	0.04	0.100	11 †

* The 1-direction corresponds to radial axis, the 2-direction corresponds to the filament length, and the 3-direction completes a right-handed orthogonal set (see Fig. 2).

† It is assumed that Case 3 is transverse-isotropic, because only the coefficients E_2, E_3, G_{23}, μ_{23}, and μ_{32} are available.

TABLE 4. *Elastic constants of the layers of the cell wall (E and G in units of 10^{11} dynes/cm^2)*

Case	Layer	E_1	E_2	E_3	G_{12}	G_{13}	G_{23}	μ_{12}	μ_{13}	μ_{23}
1	$M+P$	0.22765	0.59777	0.22578	0.07415	0.09471	0.07092	0.10079	0.18853	0.20425
1	$S_1S_2S_3$	0.83588	3.09170	0.58245	0.06137	0.15161	0.04208	0.02789	0.15885	0.11425
2	$M+P$	0.28215	3.24450	0.23567	0.10001	0.07145	0.07311	0.27527	0.02380	0.27867
2	$S_1S_2S_3$	1.41660	17.03000	0.77241	0.04535	0.16847	0.05539	0.00498	0.15831	0.10305
3	$M+P$	0.44601	1.5295	0.37308	0.10980	0.12651	0.10980	0.09570	0.17893	0.20499
3	$S_1S_2S_3$	0.39908	7.44880	0.39370	0.17621	0.20013	0.17621	0.02590	0.17760	0.20581

The elastic constants of each of the layers with respect to their principal axes (Fig. 2) are listed in Table 4. The elastic compliances of the various layers with respect to the geometric axes (see Fig. 1) can be easily obtained by using tensor transformations. The numerical calculation is straightforward and hence is not given here. With these elastic compliances and radius of each layer known, the stresses were calculated by using equations (3)–(6). The distributions of all the stresses in the radial direction of the cell wall are plotted in Figs. 3–6, and the relative angle of twist-

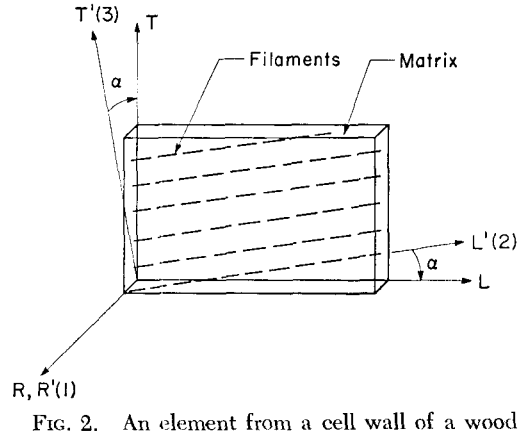

FIG. 2. An element from a cell wall of a wood fiber.

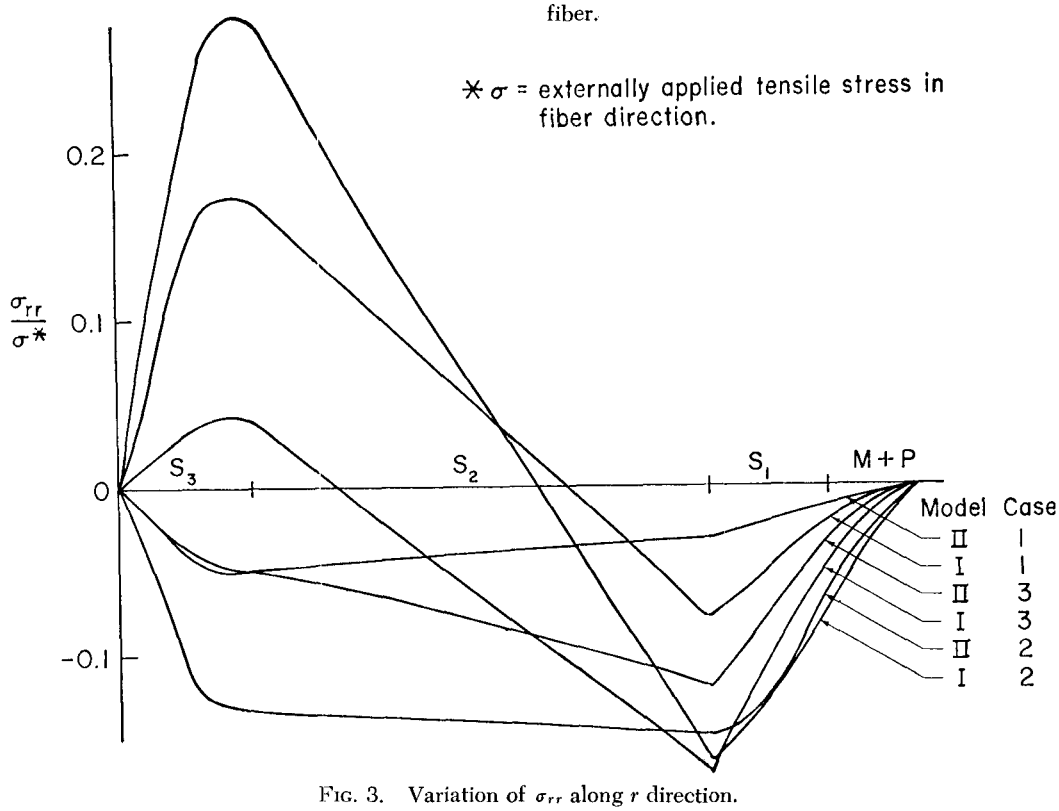

FIG. 3. Variation of σ_{rr} along r direction.

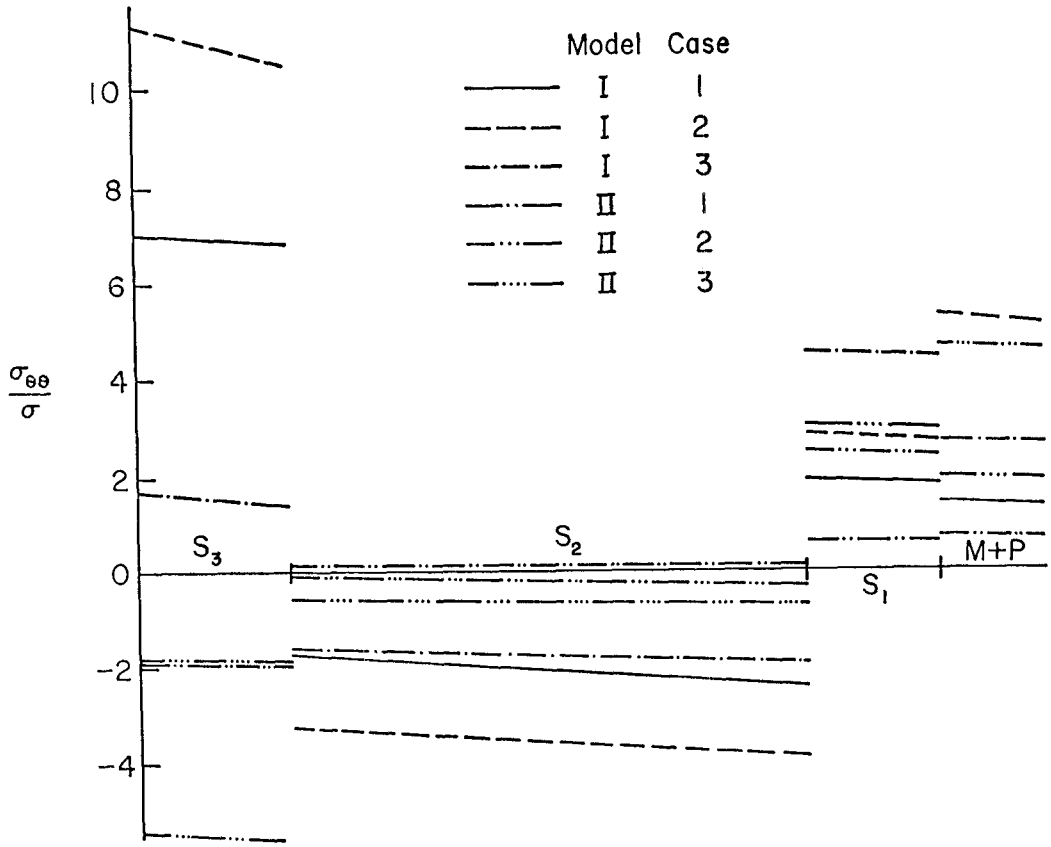

FIG. 4. Variation of $\sigma_{\theta\theta}$ along r direction.

ing of each layer is shown also. According to Lekhnitskii (1963), the total torsional rigidity (T) of a composite anisotropic cylinder equals the sum of the torsional rigidities of each layer ($T^{(j)}$); that is:

$$T = \sum_{j=1}^{n} T^{(j)},$$

The results of all cases are tabulated in Table 5.

where n is the total number of layers in the cylinder. Hence, the total relative angle of twist of a single fiber can be expressed as

$$D_{\text{total}} = \frac{\sum_{j=1}^{4} T^{(j)} D^{(j)}}{\sum_{j=1}^{4} T^{(j)}}. \qquad (21)$$

TABLE 5. *Theoretical values of the relative angle of twist of two model fibers*

		Relative angle of twist (degrees/cm)				
Model	Case	S_3	S_2	S_1	$M+P$	Single fiber
I	1	645.94	63.13	147.67	329.26	110.90
	2	787.47	57.02	186.06	122.77	103.02
	3	567.52	357.65	88.81	228.05	334.78
II	1	150.53	158.30	191.99	428.08	193.17
	2	12.92	31.83	106.85	70.50	41.79
	3	252.81	59.97	57.97	148.86	89.14

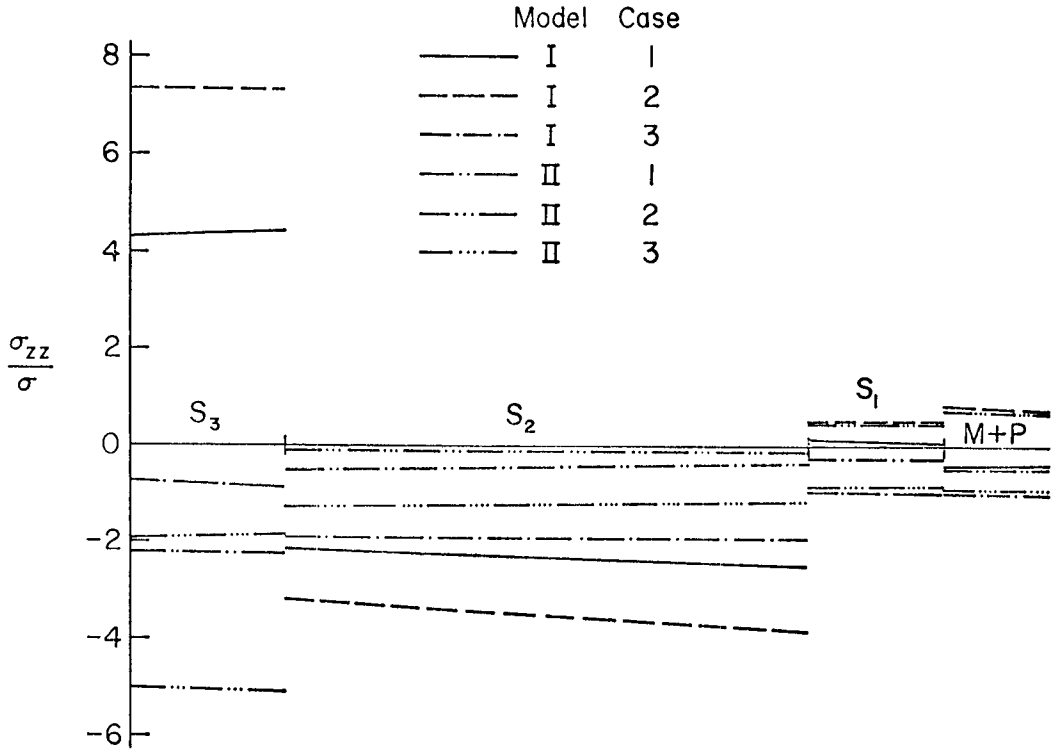

FIG. 5. Variation of σ_{zz} along r direction.

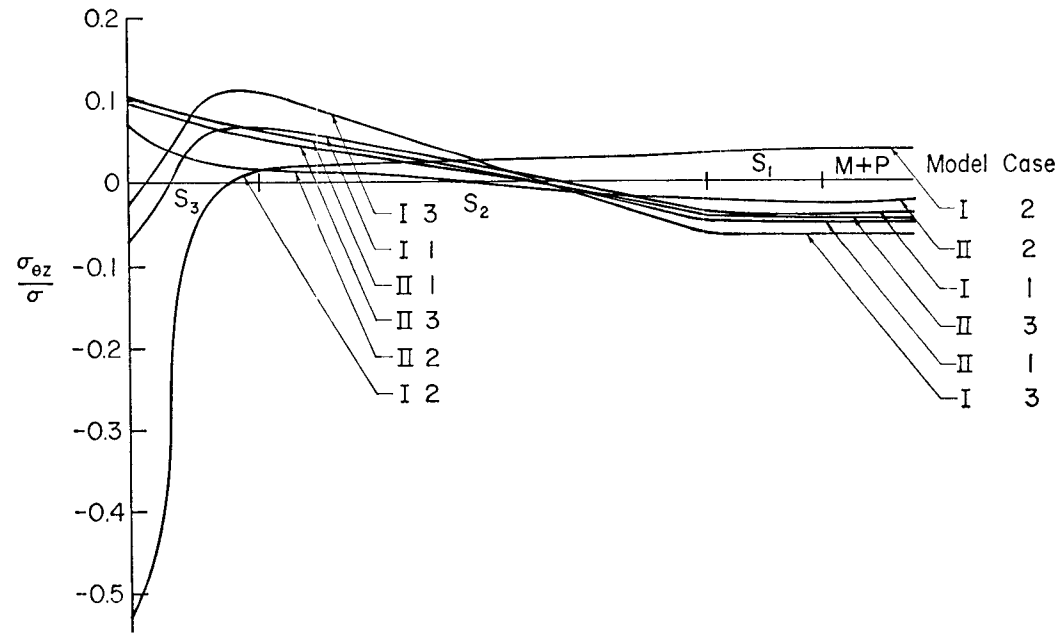

FIG. 6. Variation of $\sigma_{\theta z}$ along r direction.

TABLE 6. *Comparison of the results of stresses from two- and three-dimensional analyses*

	Three-dimensional analysis								Mark and Gillis (1970) Two-dimensional analysis			
	$\sigma_{L/\sigma}$		$\sigma_{T/\sigma}$		$\sigma_{R/\sigma}$		$\sigma_{LT/\sigma}$					
	Max	Min	Max	Min	Max	Min	Max	Min	$\sigma_{L/\sigma}$	$\sigma_{T/\sigma}$	$\sigma_{R/\sigma}$	$\sigma_{LT/\sigma}$
Tangential Wall												
$M+P$	−0.940	−0.945	2.673	2.636	0	−0.043	−0.062	−0.063	−0.203	0.141	—	0
S_1	−0.907	−0.908	4.492	4.344	−0.043	−0.172	−0.060	−0.062	−0.927	0.269	—	±0.037
S_2	−1.921	−1.936	−1.657	−1.960	0.040	−0.172	0.115	−0.060	2.613	−0.019	—	0.069
S_3	−0.757	−0.819	1.712	1.436	0.040	0	0.115	−0.029	2.061	0.026	—	0.094
Radial wall												
$M+P$	−0.864	−0.860	1.964	1.990	0	−0.032	−0.041	−0.042	−0.276	0.138	—	0
S_1	−0.845	−0.846	3.071	2.970	−0.032	−0.120	−0.039	−0.041	−1.258	0.264	—	±0.040
S_2	−1.186	−1.311	−0.584	−0.750	−0.049	−0.120	0.056	−0.039	1.543	0.035	—	0.111
S_3	−1.891	−1.915	−1.927	−1.984	0	−0.049	0.094	0.056	−0.531	0.204	—	0.092

Applying the law of mixture with the values given in Table 5, the values of the relative twisting angle of a single fiber with area percentages of tangential wall and radial wall as shown in Table 1 were calculated. The angles of relative twisting were as follows:

Case 1: 121.24°
Case 2: 95.72°
Case 3: 283.60°

These calculations contrast with the experimental data reported by Mark and Gillis (1970) of 317.70°; an average of six tests.

To illustrate the difference between two- and three-dimensional analyses, the ratios of longitudinal stress σ_L, tangential stress σ_T, radial stress σ_R, and the shear stress σ_{LT} to the externally applied tensile stress σ in the fiber direction for cases I3 and II3, along with values from two-dimensional analysis reported by Mark and Gillis (1970), are listed in Table 6. It is evident from this comparison that the three-dimensional models employed here convey a much different impression of the state of stress in the cell wall than two-dimensional models reported in the literature to date.

CONCLUSIONS

The maximum radial stress for cases I1, I2, and II1 occurred at the boundary of the S_2 and S_3 layers, while in cases I3, II2, and II3 it is at the boundary of the S_1 and S_2 layers. It should be noted here that the radial stress cannot be obtained from a two-dimensional analysis. In most cases, the tangential stresses are at a maximum in the S_3 layer except in cases I3 and II3, where it occurs in the S_1 layer. Previous studies of two-dimensional analyses of the elastic behavior of the wood fiber have led to the conclusion that the tangential stress in the cell wall is always at a maximum in the S_1 layer.

The points of zero shear stress in all cases occurred either inside the S_2 layer or inside the S_3 layer. All previous two-dimensional analyses of the stress on the cell wall reported that shear stress does not exist in the $M+P$ layer. This is in contrast to the three-dimensional analysis. In addition, it is known that shear stress exists in all radial directions of an anisotropic tube when it is subjected to a tensile force (Lekhnitskii, 1963).

These results suggest that a two-dimensional analysis is neither sufficient nor dependable for the study of elastic models of the cell-wall. Two-dimensional analysis supplies no information about the relative twisting angle of a single fiber and each layer in the cell wall, whereas three-dimensional analysis does. It can be seen from Table 5 that in case 1, model II gives the upper bound of the relative twisting angle of a single fiber, while model I gives the lower bound. This situation is reversed in cases 2 and 3. It is particularly interesting to point out that the experimental value of the relative twisting angle of a single fiber

obtained by Mark and Gillis (1970) falls within the bounds of case 3, in which the elastic constants of cellulose and matrix given by them have been used. Hence, one can conclude that three-dimensional analysis offers a more complete and rigorous solution of the elastic behavior of the wood fiber.

REFERENCES

CAVE, I. D. 1968. The anisotropic elasticity of the plant cell wall. Wood Sci. Technol., **2**(4): 268–278.

———. 1969. The longitudinal Young's modulus of *Pinus radiata*. Wood Sci. Technol., **3**(1):40–48.

GILLIS, P. P. 1969. Effect of hydrogen bonds on the axial stiffness of crystalline native cellulose. J. Polymer Sci., **A–2**(7):783–794.

———. 1970. Elastic moduli for plane stress analyses of unidirectional composites with anisotropic rectangular reinforcements. Fibre Sci. Tech., **2**:193–210.

———, R. E. MARK, AND R. C. TANG. 1969. Elastic stiffness of crystalline cellulose in the folded-chain solid state. J. Mater. Sci., **4**: 1003–1007.

JASWON, M. A., P. P. GILLIS, AND R. E. MARK. 1968. The elastic constants of crystalline native cellulose. Proc. Roy. Soc. (London), **Ser. A 306**:389–412.

LEKHNITSKII, S. G. 1963. Theory of elasticity of an anisotropic elastic body. Holden-Day, Inc., San Francisco.

LYONS, W. J. 1959. Theoretical value of the dynamic stretch moduli of cellulose. J. Appl. Phys., **30**:796–797.

MARK, R. E. 1967. Cell-wall mechanics of tracheids. Yale Press, New Haven.

———, AND P. P. GILLIS. 1970. New models in cell-wall mechanics. Wood and Fiber, **2**(2): 79–95.

———, P. N. KALONI, R. C. TANG, AND P. P. GILLIS. 1969. Solid mechanics and crystal physics as tools for cellulose structure investigation. Textile Res. J., **39**(3):203–212.

MEREDITH, R. 1946. The elastic properties of textile fibers. J. Textile Inst., **37**:469–480.

SAKUSADA, I., Y. NUKUSHINA, AND T. ITO. 1962. Experimental determination of the elastic modulus of crystalline regions in oriented polymers. J. Polymer Sci., **57**:651–660.

SCHNIEWIND, A. P. 1969. Elastic behavior of the wood fiber. *In* B. A. Jayne [ed], Theory and design of wood and fiber composite materials. University of Washington, Seattle.

TRELOAR, L. R. G. 1960. Calculation of elastic moduli of polymer crystals III: Cellulose. Polymer, **1**(3):290–303.

———, AND J. D. BARRETT. 1969. Cell-wall model with complete shear restraint. Wood and Fiber, **1**(3):205–214.

TANG, R. C., AND S. F. ADAMS. 1970. Stresses in a rotating cylinder and variable thickness disk of anisotropic materials. J. Compos. Mater., **4**:419–421.